Fall 2019

Practical methods for source separation in EMC measurements

Yuanzhuo Liu

Department:

PRACTICAL METHODS FOR SOURCE SEPARATION IN EMC MEASUREMENTS

by

YUANZHUO LIU

A THESIS

Presented to the Faculty of the Graduate School of the

MISSOURI UNIVERSITY OF SCIENCE AND TECHNOLOGY

In Partial Fulfillment of the Requirements for the Degree

MASTER OF SCIENCE IN ELECTRICAL ENGINEERING

2019

Approved by:

Jun Fan, Advisor
Victor Khilkevich
Chulsoon Hwang

PUBLICATION THESIS OPTION

This thesis consists of the following two articles, formatted in the style used by the Missouri University of Science and Technology:

Paper I: Pages 4-23 have been published by 2019 IEEE International Symposium on Electromagnetic Compatibility, Signal & Power Integrity (EMC+SIPI).

Paper II: Pages 24-38 have been published by 2019 IEEE International Symposium on Electromagnetic Compatibility, Signal & Power Integrity (EMC+SIPI).

ABSTRACT

Electromagnetic emission is critical in the electronic industry with the rapid growth of the development of the electronic device. To identify the emission from the multipule sources, two methods are proposed in the near field scan and total radiated power measurement respectively.

The first method can be applied in the measurement of the field generated by multiple non-correlated sources. The contribution of each source is determined using a blind source separation (BSS) technique. The measurements are performed using one scanning probe and stationary reference probes, avoiding the need to measure the spatial correlations of the random field. The resolving result can be used to localize the emission sources and their contribution to the far-field pattern. The method was tested on different signals with amplitude and frequency modulation.

Another method for the total radiated power (TRP) measurement of multiple non-correlated emission sources in a reverberation tent is proposed. The method can resolve the contributions of each source, which is critical for noise source identification in complex electronic systems. Blind source separation (BSS) is implemented in relatively short periods to avoid the influence of the stirring of the reverberation tent. The BSS results can be resolved to the TRP of the individual sources through an averaging cancellation method. The method might be useful in situations when no direct access to the sources is possible or desirable to obtain a signal reference and all measurement probes should be placed in the far-field zone.

ACKNOWLEDGMENTS

I would like to sincerely express my gratitude to Dr. Jun Fan and Dr. Victor Khilkevich for teaching me great skills in doing research and giving me encouraged instructions and directions when I overcome the difficulties. I learnt a lot from them, not only in the technical side, but also the non-technical side. Being the student of the two teachers is my great fortune.

Additionally, I would like to thank all the other faculty as well as all the members from the Electromagnetic Compatibility Laboratory of Missouri University of Science and Technology. It has been a great pleasure to be a member of the lab. Whenever I need help, they reach out to me without hesitation, not only in research but also in the life. It's my pleasure to work with all of you.

Finally, I would like to thank my parents for supporting and encouraging me to pursue my academics unconditionally along the way. I'm proud to be their child.

TABLE OF CONTENTS

LIST OF ILLUSTRATIONS

PAPER I Page

PAPER II

LIST OF TABLES

PAPER II Page

1. INTRODUCTION

Electromagnetic emission has been receiving increasing attention to the rapid growth of the electronic industry. Consequently, electronic equipment and systems become more susceptible to electromagnetic interference (EMI). To deal with the electromagnetic interference (EMI) caused by the noise, it is of critical importance to identify the emission sources. In complex electronic systems, noise is a product of multiple, often uncorrelated, emission. In a situation with multiple sources knowing the contributions of the individual sources might help to solve the emission problems.

Near-field scanning (NFS) is a widely used technique to characterize and localize the radiation sources in the complex electronic environment accurately and reliably. The NFS measurements can be used to estimate the far-field pattern and identify the radiating sources with the assistance of the emission source microscopy (ESM) technique. However, due to the increased functionality and the circuit density of the electronic devices, it is usually hard to resolve the individual radiating sources with the help of NFS if the phase information is missing. Therefore, the ability to measure the amplitude and the phase of the electromagnetic fields is of critical importance.

A method that uses two moving probes for NFS has been developed for complete characterization of stochastic fields (the phase information is contained in the spatial correlation function of the fields), which is, however, very time consuming and requires large computational resources.

To reduce the measurement time and to avoid measuring spatial correlations, a signal resolving method was proposed which requires placing reference probes near the actual sources of radiation and canceling contributions of all other sources.

Another critical EMC measurement is total radiated power. In many circumstances, the electronic equipment may be extremely complicated or compact such that it is difficult or impossible to place the reference probe close to the radiation sources. A new method is proposed in this paper so that all probes can be placed far away from the sources such that no access to the sources to obtain the reference signals is required. The complexity of the measurement and data processing time are consequently reduced.

In Paper I, a method for the total radiated power measurement of multiple non-correlated emission sources in the reverberation tent is proposed. Reverberation chambers, in general, are widely used as established environments to perform electromagnetic susceptibility and emission measurements . A well-stirred reverberation chamber emulates a statistically uniform and isotropic field within its working volume, providing a simple, cheap, and effective way to measure the total radiated power.

In order to resolve the contributions of the individual sources in the multi-sourced environment, a BSS-based method is introduced. Blind source separation deals with recovering a set of underlying sources from an unknown mixture.

Application of the BSS to separate signals in a conventional reverberation chamber with the discrete and well-controlled movement of the stirrer is straightforward (since for each position of the stirrer, the chamber represents a time-invariant system). However, in recent years, reverberation tents are gaining popularity due to their low cost and ease of use. In the reverberation tents, the mode stirring is performed by random

shaking of the tent's walls, and the entire measurement setup is inherently time-variant. The intent of this paper is to investigate the possibility of using BSS to separate signals and eventually measure their TRP contributions in a reverberation tent.

PAPER

I. SCANNING OF RANDOM FIELDS USING BLIND SOURCE SEPARATION

Yuanzhuo Liu, Jiangshuai Li, Shaohui Yong, Ruijie He, Victor Khilkevich

EMC Laboratory, Missouri University of Science and Technology

Rolla, MO, 65409

ABSTRACT

A method for the measurement of the field generated by multiple non-correlated sources is proposed. The contribution of each source is determined using a blind source separation (BSS) technique. The measurements are performed using one scanning probe and stationary reference probes, avoiding the need to measure the spatial correlations of the random field. The resolving result can be used to localize the emission sources and their contribution to the far-field pattern. The method was tested on different signals with amplitude and frequency modulation.

1. INTRODUCTION

With the rapid development of modern electronic devices, the operating data rate continues to rise. Consequently, electronic equipment and systems become more susceptible to electromagnetic interference (EMI). Near-field scanning (NFS) is a widely used technique to characterize and localize the radiation sources in the complex

electronic environment accurately and reliably [1-8]. The NFS measurements can be used to estimate the far-field pattern and identify the radiating sources with the assistance of the emission source microscopy (ESM) technique [9- 12]. However, due to the increased functionality and the circuit density of the electronic devices, it is usually hard to resolve the individual radiating sources with the help of NFS if the phase information is missing [13]. Therefore the ability to measure the amplitude and the phase of the electromagnetic fields is of critical importance.

A method that uses two moving probes for NFS has been developed for complete characterization of stochastic fields (the phase information is contained in the spatial correlation function of the fields), which is, however, very time consuming and requires large computational resources [14]. To reduce the measurement time and to avoid measuring spatial correlations, a signal resolving method was proposed which requires placing reference probes near the actual sources of radiation and canceling contributions of all other sources [15, 16].

However, in many circumstances, the electronic equipment may be extremely complicated or compact such that it is difficult or impossible to place the reference probe close to the radiation sources. A new method is proposed in this paper so that all probes can be placed far away from the sources such that no access to the sources to obtain the reference signals is required. The complexity of the measurement and data processing time are consequently reduced.

The paper is organized as follows. Section 2 introduces the BSS method. In Section 3 the signal cancellation method is explained. Section 4 describes measurements

in both frequency and time domains including amplitude and frequency modulation and demonstrates the separation results. Finally, the conclusions are given in Section 5. .

2. BLIND SOURCE SEPARATION INTRODUCTION

BSS is intended to be used in situations when only the mixed signals can be accessed rather than the individual ones. With the help of BSS, the source signals can be recovered from the linear combination using certain information about the nature of the signals without any knowledge about the mixing process.

In general, blind source separation can be formulated as a generalized eigenvalue decomposition under certain assumptions, for instance, non-Gaussian, non-stationary independent sources[15] .

The problem of the source separation is applied to the signal mixture which is defined as:

$$\mathbf{X} = \mathbf{AS} \tag{1}$$

where **X** is the multi-dimensional matrix containing mixed signals, **A** is the mixing matrix and the **S** is the source matrix. If the inverse matrix of **X** is available, the sources **S** can therefore be recovered.

The BSS therefore can simply be implemented in two steps. First is to compute the unmixing matrix **W** with generalized eigenvalue procedure. Then the sources can be recovered as:

$$\mathbf{W} = \mathrm{Eig}(\mathbf{X} \cdot \mathbf{X}^{H}, \mathbf{Q} \tag{2}$$

$$\hat{\mathbf{S}} = \mathbf{W}^{H}\mathbf{X} \tag{3}$$

Here **Q** is a diagonal cross-statistic that differs for different assumptions, H – is the conjugate transpose operator, and $\hat{\mathbf{S}}$ is a scaled (by unknown complex numbers) and permuted version of **S**.

In [17], it is derived that for the non-white and non-correlated sources, **Q** is the symmetric cross-correlation for time-delayed:

$$\mathbf{Q} = \mathbf{X}(0 \dots T-\tau) \cdot \mathbf{X}^H(\tau+1 \dots T) + \mathbf{X}(\tau+1 \dots T) \cdot \mathbf{X}^H(1 \dots T-\tau) \qquad (4)$$

where τ is the delay within the non-zero autocorrelation interval of the source signals and T is the observation interval. Statistics (4) is used throughout the rest of the paper to perform the signal separation.

The workflow of the procedure is demonstrated in Figure 1.

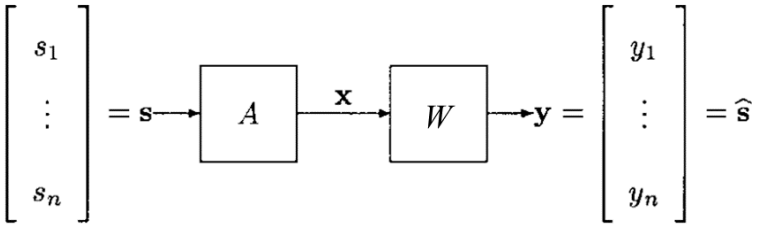

Figure 1. Flow diagram of the BSS process.

The actual source signals can be resolved from $\hat{\mathbf{S}}$ by the averaging cancellation method described in the next section.

3. SIGNAL CANCELLATION METHOD

A signal cancellation method based on averaging over realizations can be applied to separate multiple non-correlated sources. Suppose two non-correlated sources create electromagnetic field and two probes are used to sample the field (this simple case can be easily generalized to a situation of n sources and n probes). On account of the linearity of Maxwell's equations the outputs of the probes (in frequency domain) are linear combinations of the sources as is shown in Figure 2.

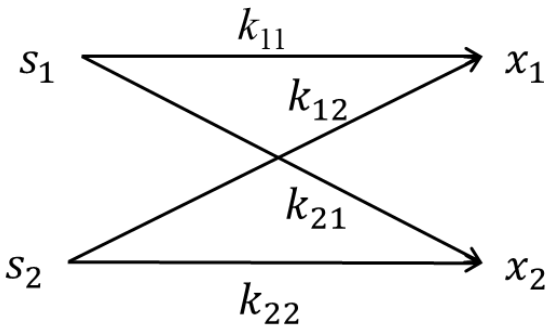

Figure 2. Relation between the source and output signals.

Here s_1 and s_2 are the signals at a certain frequency, x_1 and x_2 are the probe output signals, k_{ij} are the transfer functions which depend on the position of the sources and probes. Therefore, the output can be expressed as:

$$x_1 = k_{11}\, s_1 + k_{12}\, s_2 \tag{5}$$

$$x_2 = k_{21}\, s_1 + k_{22} \tag{6}$$

Suppose that the probe 2 is coupled to the source 1 only (such that $k_{22} = 0$), in other words, the probe 2 is a reference probe for the signal 1. Then the ratio of the probe output signals is:

$$\frac{x_1}{x_2} = \frac{k_{11}s_1 + k_{12}s_2}{k_{21}s_1} = \frac{k_{11}}{k_{21}} + \frac{k_{12}s_2}{k_{21}s_1} \tag{7}$$

In [17], it is demonstrated that if s_1 and s_2 are random variables with bounded and symmetrical distributions, the expected value of the ratio s_2/s_1 is zero. Then the expected value of the ratio x_1 / x_2 is equal to k_{11} / k_{21}:

$$\left\langle \frac{x_1}{x_2} \right\rangle = \frac{k_{11}}{k_{21}} + \frac{k_{12}}{k_{21}} \left\langle \frac{s_2}{s_1} \right\rangle = \frac{k_{11}}{k_{21}} \tag{8}$$

The phase of the ratio k_{11} / k_{21} is the phase difference between the contribution of the source 1 to the field at the location of the probe 1 and the reference probe signal:

$$\Delta\varphi_1 = \arg\left(\frac{k_{11}}{k_{21}}\right) \tag{9}$$

This phase difference can be used simply as a phase of the field contribution of the source 1, since the initial phase is usually irrelevant (see [17] for details).

The amplitude of the contribution can be determined as follows. Let us define the averaged amplitude of the contribution for the source 1 to the field at the probe location 1 as:

$$A_1 = \langle |k_{11}s_1| \rangle \tag{10}$$

If, as was assumed earlier, $k_{22} = 0$, using (6) s_1 can be expressed as

$$s_1 = \frac{x_2}{k_{21}} \tag{11}$$

Combining (10) and (11) the averaged amplitude can be written as follows:

$$A_1 = \left\langle \left| \frac{k_{11}x_2}{k_{21}} \right| \right\rangle = \langle |x_2| \rangle \left| \left\langle \frac{x_1}{x_2} \right\rangle \right| \tag{12}$$

Finally, using (8) the averaged amplitude is obtained as:

$$A_1 = \langle |x_2| \rangle \left| \left\langle \frac{x_1}{x_2} \right\rangle \right| \tag{13}$$

Therefore, formulas (8) and (13) can be used to obtain the amplitude and phase of the field contributions if the reference signals are available. The reference signals can be obtained from x_1 and x_2 by applying the BSS procedure (2), (3). However, as mentioned above the BSS would produce the scaled signals:

$$\begin{aligned} \hat{s}_1 &= a_1 s_1 \\ \hat{s}_2 &= a_2 s_2 \end{aligned} \tag{14}$$

where a_1 and a_2 are unknown scaling coefficients. Notice that the amplitude in (13) does not depend on the coefficient k_{21}, or any other scaling coefficient in the reference probe channel. Because of this, the separated references (14) can be directly used to calculate the averaged amplitudes of the field contributions due to both sources in, for example, probe 1 as

$$\begin{aligned} A_1 &= \langle |\hat{s}_1| \rangle \left| \left\langle \frac{x_1}{\hat{s}_1} \right\rangle \right| \\ A_2 &= \langle |\hat{s}_2| \rangle \left| \left\langle \frac{x_1}{\hat{s}_2} \right\rangle \right| \end{aligned} \tag{15}$$

However according to (9) the phase of the field contribution depends on the scaling coefficient in the reference channel, and if the separated signals (14) are directly used as references, the phase of the field contribution also becomes unknown:

$$\Delta\varphi_1 = \arg\left(\frac{k_{11}}{a_1}\right) \tag{16}$$

So, the scaling of the separated signals $\hat{\mathbf{S}}$ should be dealt with. This is achieved by the calculation of the following ratios:

$$\begin{aligned}\left\langle \frac{x_1}{\hat{s}_1} \right\rangle &= \frac{k_{11}}{a_1} \\ \left\langle \frac{x_1}{\hat{s}_2} \right\rangle &= \frac{k_{12}}{a_2} \\ \left\langle \frac{x_2}{\hat{s}_1} \right\rangle &= \frac{k_{21}}{a_1} \\ \left\langle \frac{x_2}{\hat{s}_2} \right\rangle &= \frac{k_{22}}{a_2}\end{aligned} \tag{17}$$

Notice, that a general case (5), (6) is assumed here and $k_{22} \neq 0$.

Now by taking the ratios of the averages in (17), the phases of the field contributions can be obtained as:

$$\begin{aligned}\Delta\varphi_1 &= \arg\left(\frac{\left\langle \frac{x_1}{\hat{s}_1} \right\rangle}{\left\langle \frac{x_1}{\hat{s}_2} \right\rangle}\right) = \arg\left(\frac{k_{11}}{k_{12}}\right) \\ \Delta\varphi_2 &= \arg\left(\frac{\left\langle \frac{x_2}{\hat{s}_1} \right\rangle}{\left\langle \frac{x_2}{\hat{s}_2} \right\rangle}\right) = \arg\left(\frac{k_{21}}{k_{22}}\right)\end{aligned} \tag{18}$$

I.e. the phase differences independent on the unknown scaling coefficients can be determined.

To summarize, the procedure described above is applied in the following sequence:

1. The signals in two probe channels are separated using the BSS to obtain scaled reference signals (14).

2. The amplitudes of the source contributions are calculated using (15).

3. The phases of the contributions are calculated using (18).

4. To perform the field scan one of the probes is moved over the DUT and the other one is used as a stationary reference probe.

The proposed measurement procedure is validated in the following section.

4. MEASUREMENTS AND RESULTS

4.1. INTRODUCTION OF THE MEASUREMENT SETUP

The measurement is designed as shown in Figure 3. Two RF signal generators provide non-correlated source signals. A two-channel arbitrary signal generator is used to add modulation to the sources if needed. Two loop antennas (DUT) mounted on a metal plane are the emission sources. Two log-periodic antennas are used as measurement probes. One antenna is fixed as a reference antenna and the other one can move along a certain direction for scanning.

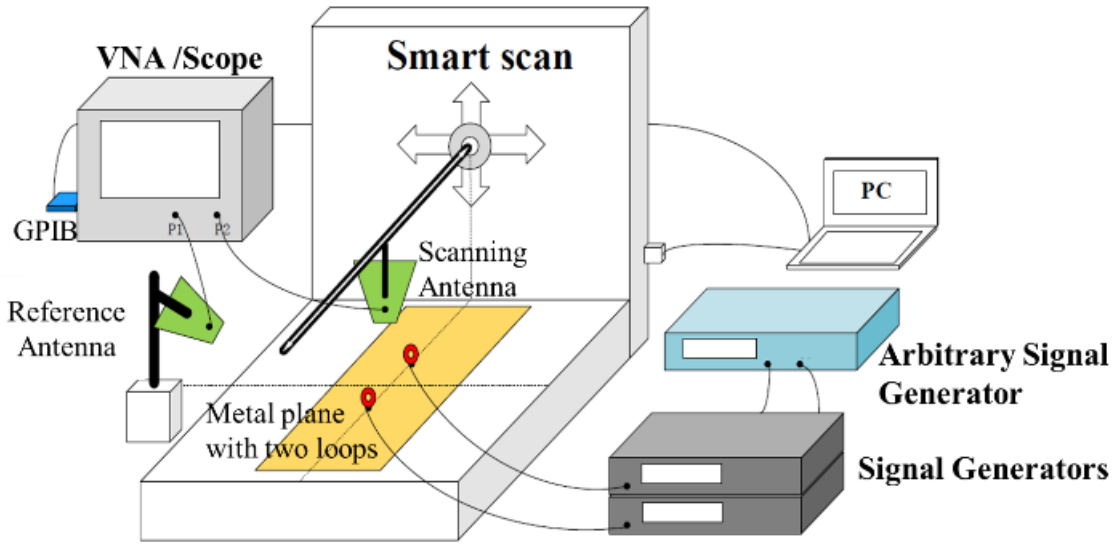

Figure 3. General measurement setup.

A portable computer (PC) controls the scanning machine and obtains data from the measurement instrument (VNA or oscilloscope). For each position of the scanning

antenna, the VNA/scope will proceed one sweep/acquisition simultaneously in two channels.

To verify the result, the contributions of the individual sources are also measured directly by turning off the other source.

4.2. 1D SCANNING

4.2.1. Frequency Domain. For a 1D scanning, the field is measured at 50 positions along a line of 490 mm long at approximately 20 cm above the DUT. A VNA in a tuned receiver mode is used as a measurement instrument. Source 1 produces a 2.9 GHz signal and source 2 produces a 2.8995 GHz signal (the frequency difference is introduced only to facilitate visual identification of signals by the rate of change of the phase progression; since the generators are not synchronized to the same reference, the signals they produce are non-correlated for any nominal frequency difference). The frequency difference of the two sources is within the IF bandwidth of the VNA such that the signals ate indistinguishable in the frequency domain. The VNA is tuned to 2.9 GHz and performs a zero-span sweep at each position of the scanning antenna and the averaging needed to determine the amplitudes and phases in (15) and (18) is performed over multiple sweeps.

The cases are investigated:

1. Pure sinusoidal carriers.

2. Carriers modulated by noise signals (frequency modulation, 1 MHz frequency deviation, uncorrelated modulation signals for both carriers).

3. Carriers modulated by pulse signals (amplitude modulation, 20 Hz signal with 12% duty cycle for carrier 1, and 30 Hz signal with 8% duty cycle for carrier 2).

Figure 4 gives examples of mixed signals measured at a certain scan antenna position. The X-axis represents the number of the sweep sample, and the Y-axis represents the amplitude and phase of the signals.

For each of the scanning positions, the signals are separated using (3), (4) and the contributions are calculated according to (15) and (18). Resulting phases and averaged amplitudes are presented in Figure 5 as a function of the coordinate of the scanning probe in comparison with the directly measured quantities. In the figure the lines A and B mark the positions of the two sources.

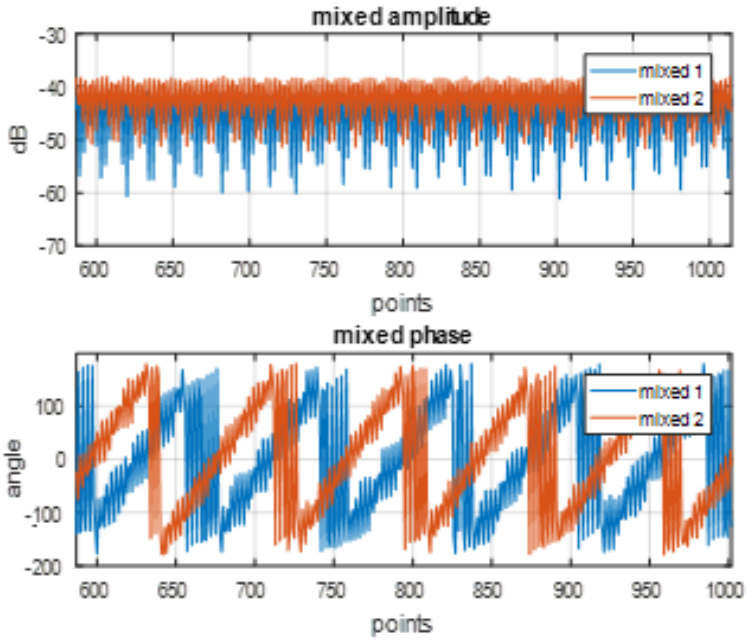

(a) Case 1: pure sine

Figure 4. Examples of mixed signals measured in frequency domain.

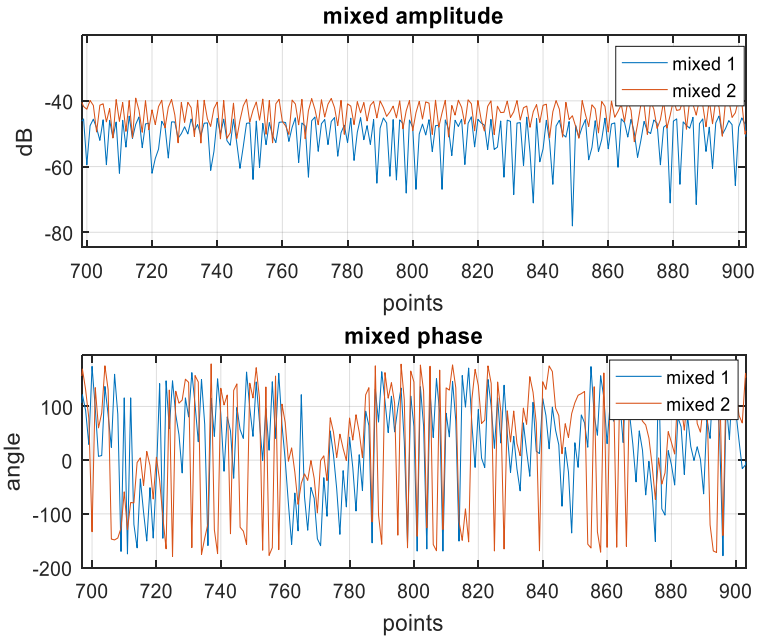

(b) Case 2: External FM noise

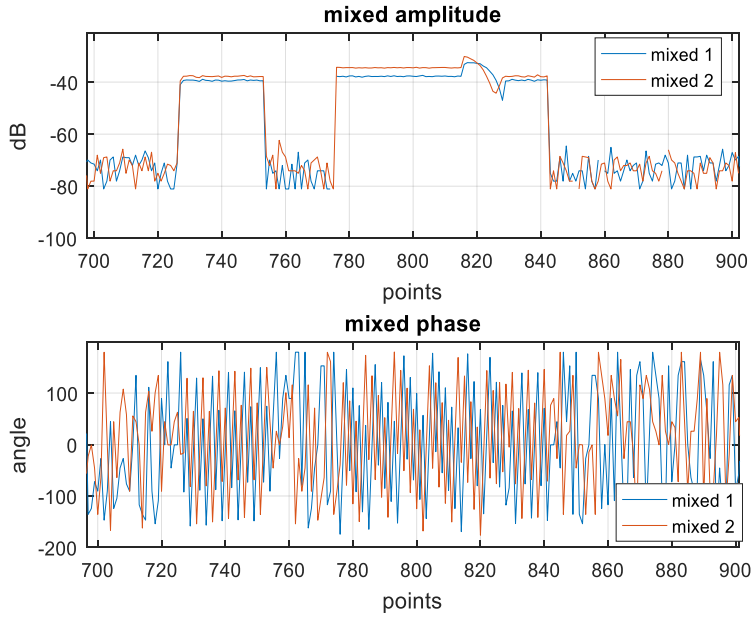

(c) Case 3: Pulse

Figure 4. Examples of mixed signals measured in frequency domain (cont.).

As can be seen the resolved amplitudes and phases match very well with the directly measured quantities regardless on the nature of the source signals, demonstrating that the proposed method can be used to accurately measure the contribution of sources for different kinds of signals, including random ones and pulses signals typical for digital electronic devices.

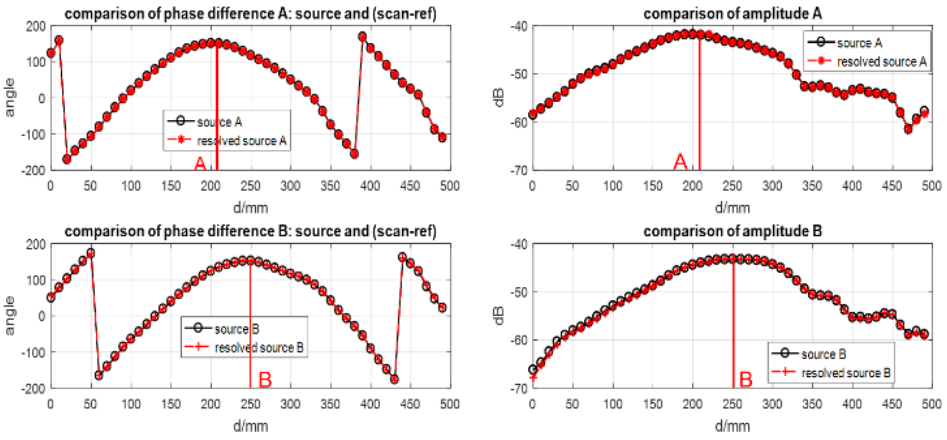

(a) Case 1: pure sine

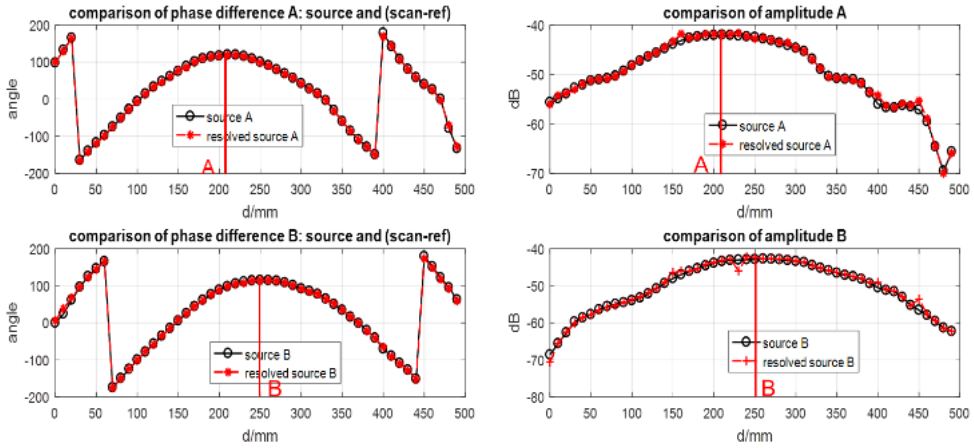

(b) Case 2: External FM noise.

Figure 5. Comparison of the resolved results and the source contributions in frequency domain measurement.

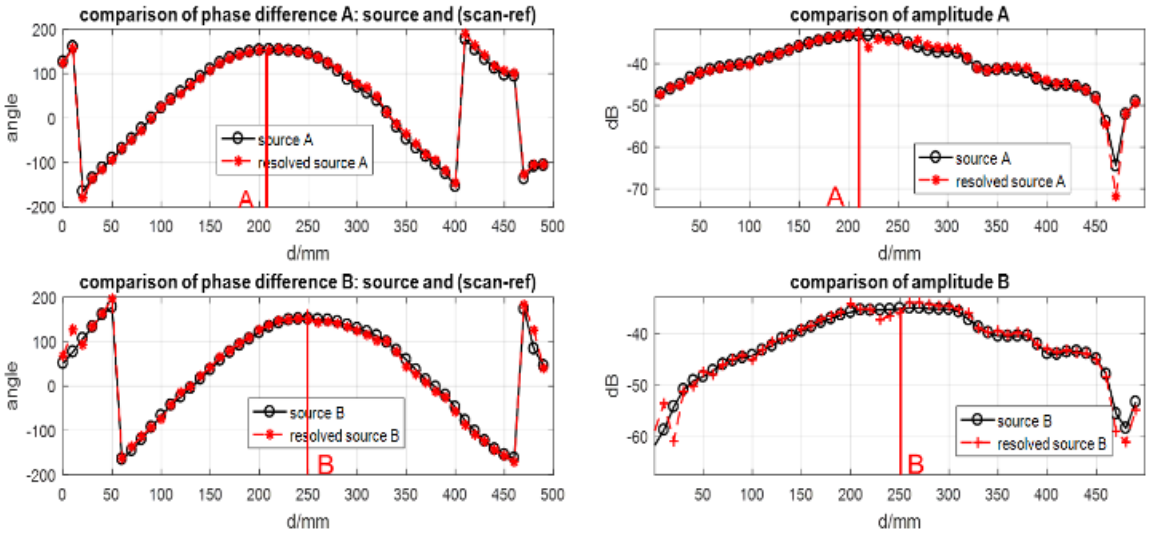

(c) Case 3: Pulse

Figure 5. Comparison of the resolved results and the source contributions in frequency domain measurement (cont.).

4.2.2. Time Domain. For the time domain measurement, an oscilloscope is used as a receiver. In this measurement source 1 produces a 1.005 GHz sinusoidal signal and source 2 produces a 1.007 GHz sinusoidal signal. The acquisition time is set to 10 μs. The record length is 1 Msa.

Compared to the frequency domain measurement, the data volume of the time domain measurement is much higher. When the original data is recorded from the scope, the data is cut into small sub-frames and the short-term FFT is performed. Values of the short-term FFT corresponding to 1 GHz are used for signal separations. The resulting curves shown in Figure 6 are very similar to the ones obtained in the frequency domain measurement matching very accurately with the directly measured amplitude and phase distributions.

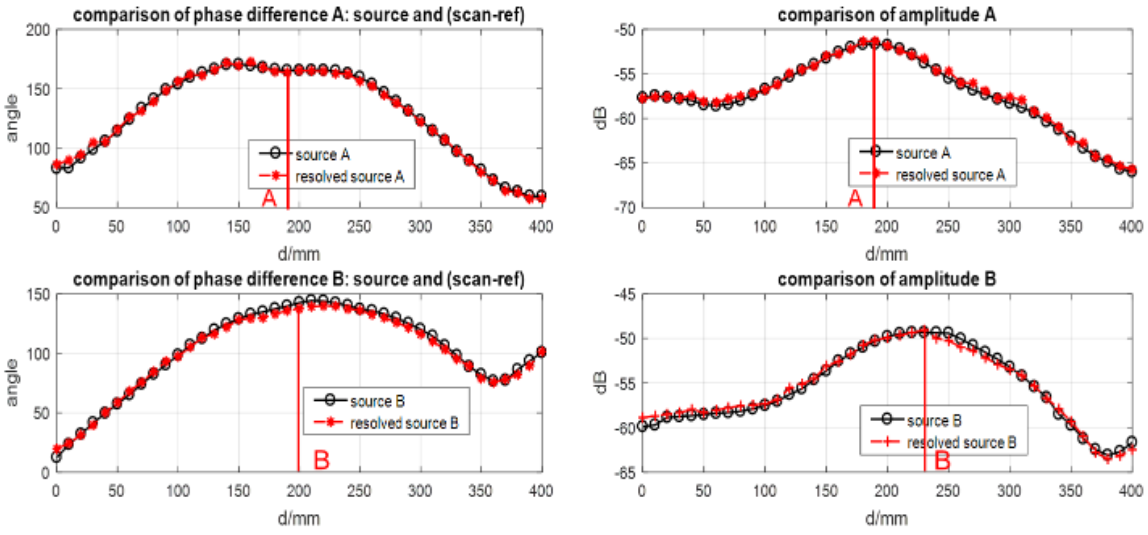

Figure 6. Comparison of the resolved results and the source sontributions in time domain measurement.

4.3. 2D SCANNING

To further demonstrate capabilities of the proposed method a 2D scanning of a $320\text{mm} \times 140\text{mm}$ area is implemented with 136 (17×8) positions in the setup in Figure 3. The measurement is performed in the frequency domain for two sinusoidal sources.

Figure 7 demonstrates the amplitude distribution obtained for the scanning channel without signal separation (i.e. average amplitude of the total field). The actual locations of the sources (loop antennas) are marked by the points A and B. As can be seen, the obtained pattern contains a large maximum and does not allow to distinguish the two sources. Whereas after applying the proposed separation method the individual amplitude contributions shown in Figure 8 reveal the actual locations of the antennas.

This example demonstrates a possibility to locate individual uncorrelated EMI sources just by observing amplitudes of their contributions to the total field. Even more

accurate localization can be potentially achieved if the proposed method is used in conjunction with the emission source microscopy (ESM) method [12], which allows using amplitude and phase distributions of the scanned fields to obtain a focused image of the radiating electromagnetic sources.

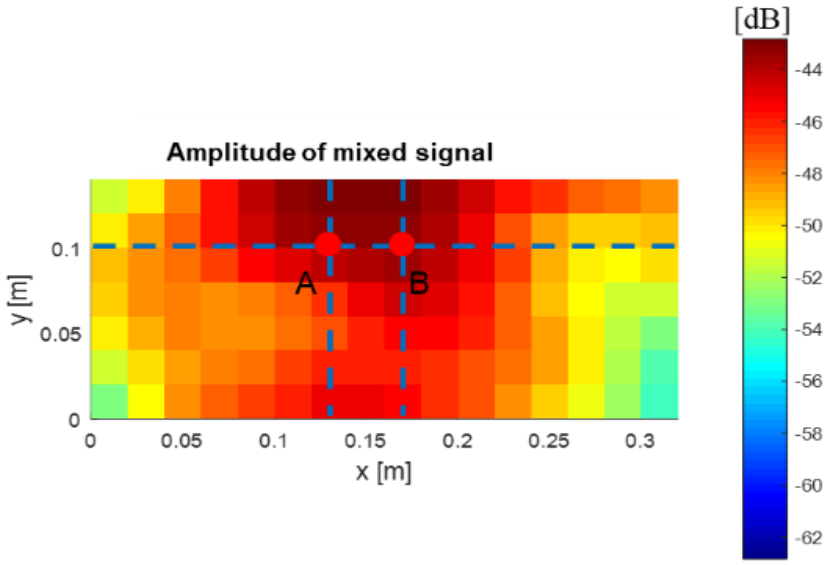

Figure 7. Averaged amplitude of the mixed signals.

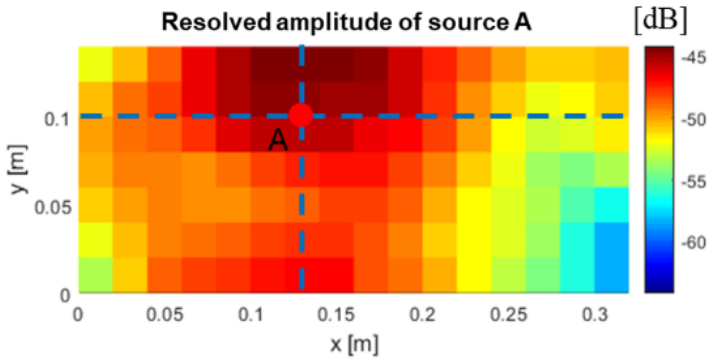

(a) Resolved contributions for source A

Figure 8. Averaged amplitude.

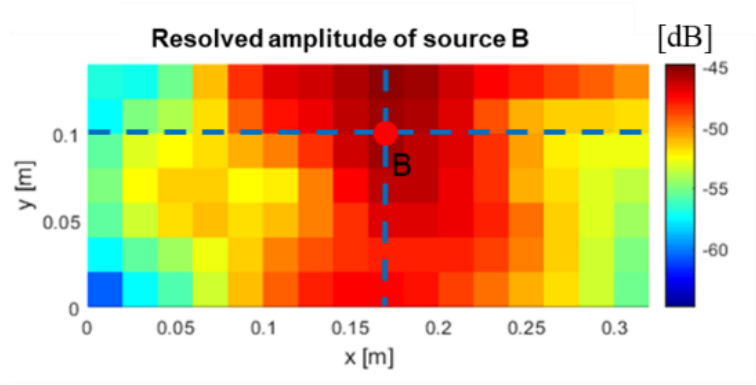

(b) Resolved contributions for source B

Figure 8. Averaged amplitude (cont.).

5. SUMMARY AND CONCLUSIONS

A method for the measurement of the field generated by multiple uncorrelated sources is proposed. The method can separate the field contributions of each source with the assistance of the BSS. The number of resolvable sources on practice is limited to the number of channels of the measurement instrument (VNA or oscilloscope). If the number of sources exceeds the number of probes the method in its current form will generally fail. However it still potentially can be used if the number of probes is equal to the number of dominant sources. The applicability and accuracy of the method in this case required additional investigation.

The advantage of the proposed method over the alternative [16] is that all probes can be placed in the far-field zone such that no access to the sources to obtain the reference signals is required.

With this method, the complexity of the measurement and the elapsed processing time are consequently reduced compared to the methods requiring to measure the spatial correlation of the random fields [17]. The resolving result can be used to localize the emission sources, as well as their contributions to the far-field pattern (see [12] for details).

The method is tested on different signals with amplitude and frequency modulation, including pure sin sources, AM/FM sources, noise modulated sources, and the pulse sources in both frequency and time domains. 2D scanning is also implemented and the contribution of the individual sources is separated successfully allowing to locate positions of the sources.

REFERENCES

[1] A. Patnaik et al., "Source isolation measurements in a multi-source coupled system," 2017 IEEE International Symposium on Electromagnetic Compatibility & Signal/Power Integrity (EMCSI), Washington, DC, 2017, pp. 75-80.

[2] Q. Huang, Y. Liu, L. Li, Y. Wang, C. Wu and J. Fan, "Radio frequency interference estimation using transfer function based dipole moment model," 2018 IEEE International Symposium on Electromagnetic Compatibility and 2018 IEEE Asia-Pacific Symposium on Electromagnetic Compatibility (EMC/APEMC), Singapore, 2018, pp. 115-120.

[3] L. Zhang et al., "Sparse Emission Source Microscopy for Rapid Emission Source Imaging," in IEEE Transactions on Electromagnetic Compatibility, vol. 59, no. 2, pp. 729-738, April 2017.

[4] Q. Huang, F. Zhang, T. Enomoto, J. Maeshima, K. Araki and C. Hwang, "Physics-based dipole moment source reconstruction for RFI on a practical cellphone", IEEE Trans. Electromagn. Compat., vol. 59, no. 6, pp. 1693-1700, Dec. 2017.

[5] Y. Liu, R. He, V. Khilkevich and P. Dixon, "Shielding Effectiveness of Board Level Shields with Absorbing Materials," 2019 IEEE International Symposium on Electromagnetic Compatibility, Signal & Power Integrity (EMC+SIPI), New Orleans, LA, USA, 2019, pp. 84-89.

[6] L. Zhang et al., "EMI Coupling Paths and Mitigation in Optical Transceiver Modules," in IEEE Transactions on Electromagnetic Compatibility, vol. 59, no. 6, pp. 1848-1855, Dec. 2017.

[7] J. Li et al., "EMI coupling paths in silicon optical sub-assembly package," 2016 IEEE International Symposium on Electromagnetic Compatibility (EMC), Ottawa, ON, 2016, pp. 890-895.

[8] Q. Huang and J. Fan,“ Machine Learning Based Source Reconstruction for RF Desense", IEEE Trans. Electromagn. Compat., vol. 60, no. 6, pp. 1640-1647, Dec. 2018.

[9] D. Nozadze et al., "Prediction of Worst-Case Radiation Immunity in Cable Harnesses," 2018 IEEE Symposium on Electromagnetic Compatibility, Signal Integrity and Power Integrity (EMC, SI & PI), Long Beach, CA, 2018, pp. 604-609.

[10] C. Hwang and Q. Huang, "IC placement optimization for RF interference based on dipole moment sources and reciprocity," IEEE Asia-Pacific Electromagn. Compat. Symp., 2017, pp.331-333.

[11] Q. Huang et al., “Desense Prediction and Mitigation from DDR Noise Source,” in Proc. of IEEE Symp. Electromagn.Compat., 2018, pp. 139-144.

[12] M. Sørensen, H. Kajbaf, V. V. Khilkevich, L. Zhang and D. Pommerenke, "Analysis of the Effect on Image Quality of Different Scanning Point Selection Methods in Sparse ESM," in IEEE Transactions on Electromagnetic Compatibility.

[13] P. Maheshwari, H. Kajbaf, V. V. Khilkevich and D. Pommerenke, "Emission Source Microscopy Technique for EMI Source Localization," in IEEE Transactions on Electromagnetic Compatibility, vol. 58, no. 3, pp. 729-737, June 2016.

[14] H. Fan, “Far field radiated emission prediction from magnetic near field magnitude-only measurements of pcbs by genetic algorithm,” in 2009 IEEE Int. Symp. on Electromagn. Compat., Aug 2009, pp. 321–324.

[15] D. W. P. Thomas et al., "Near-field scanning of stochastic fields considering reduction of complexity," 2017 International Symposium on Electromagnetic Compatibility - EMC EUROPE, Angers, 2017, pp. 1-6.

[16] A. Patnaik et al., "Source isolation measurements in a multi-source coupled system," 2017 IEEE International Symposium on Electromagnetic Compatibility & Signal/Power Integrity (EMCSI), Washington, DC, 2017, pp. 75-80.

[17] T. Li, V. Khilkevich and D. Pommerenke, "Phase-Resolved Near-Field Scan Over Random Fields," IEEE Transactions on Electromagnetic Compatibility, vol. 58, no. 2, pp. 506-511, April 2016.

[18] Lucas. Parra, Paul, Sajda., "Blind source separation via generalized eigenvalue decomposition" The Journal of Machine Learning Research, Vol. 4 Issue 7-8, October 1 - November15, 2004, Pages 1261-1269

II. MEASUREMENT OF THE TOTAL RADIATED POWER CONTRIBUTIONS IN A REVERBERATION TENT

Yuanzhuo Liu, Ruijie He, Jiangshuai Li, Victor Khilkevich

EMC Laboratory, Missouri University of Science and Technology

Rolla, MO, 65409

ABSTRACT

A method for the total radiated power (TRP) measurement of multiple non-correlated emission sources in a reverberation tent is proposed. The method can resolve the contributions of each source, which is critical for noise source identification in complex electronic systems. Blind source separation (BSS) is implemented in relatively short periods to avoid the influence of the stirring of the reverberation tent. The BSS results can be resolved to the TRP of the individual sources through an averaging cancellation method. The method might be useful in situations when no direct access to the sources is possible or desirable to obtain a signal reference and all measurement probes should be placed in the far-field zone.

1. INTRODUCTION

Electromagnetic emission has been receiving increasing attention to the rapid growth of the electronic industry. To deal with the electromagnetic interference (EMI) caused by the noise, it is of critical importance to identify the emission sources [1-9]. In

complex electronic systems, noise is a product of multiple, often uncorrelated, emission. In a situation with multiple sources knowing the contributions of the individual sources might help to solve the emission problems.

In this paper, a method for the total radiated power measurement of multiple non-correlated emission sources in the reverberation tent is proposed. Reverberation chambers, in general, are widely used as established environments to perform electromagnetic susceptibility and emission measurements [10-13]. A well-stirred reverberation chamber emulates a statistically uniform and isotropic field within its working volume [14-17], providing a simple cheap and effective way to measure the total radiated power.

In order to resolve the contributions of the individual sources in the multi-sourced environment, a BSS-based method is introduced. Blind source separation deals with recovering a set of underlying sources from an unknown mixture.

Application of the BSS to separate signals in a conventional reverberation chamber with the discrete and well-controlled movement of the stirrer is straightforward (since for each position of the stirrer the chamber represents a time-invariant system). However, in recent years reverberation tents are gaining popularity due to their low cost and ease of use [18]. In the reverberation tents, the mode stirring is performed by random shaking of the tent's walls and the entire measurement setup is inherently time-variant. The intent of this paper is to investigate the possibility to use BSS to separate signals and eventually measure their TRP contributions in a reverberation tent.

The paper is organized as follows. Section 2 introduces the methodology of the proposed method. In Section 3, the TRP measurement in the reverberation chamber is

described. Section 4 demonstrates and analyzes the resolving result. Finally, the summary and conclusions are given in Section 5.

2. METHODOLOGY

2.1. BSS INTRODUCTION

A BSS-based method is used to resolve the contributions of the non-correlated signals measured in the reverberation tent. The BSS methods were originally applied in the area of the neural network, image enhancement and biomedical signal processing, wireless telecommunication systems like sonar and radar systems [22].

In [23] the concept of BSS is proposed as a tool to identify individual signals from a mixture containing unknown, multiple and overlapping signals. The BSS can be formulated as a generalized eigenvalue decomposition under different assumptions about the source signals (for example non-Gaussian, non-stationary independent sources, and so on).

The fields in the reverberation tent obey superposition due to the linearity of Maxwell's equations. For this reason, the BSS model of the reverberation tent is formulated as a linear simultaneous mixture of signals. The observed signals represent a matrix which is related to the sources as

$$\mathbf{X} = \mathbf{AS} \tag{1}$$

where S is the matrix consisting of the original non-correlated signals and A is an unknown mixing matrix. X is the multi-dimensional matrix containing measured scalar signals x as (matrix $\mathbf{S}$ has a similar structure):

$$\mathbf{X}(0 \ldots \mathrm{T}) = \begin{pmatrix} x_1(0) & \cdots & x_1(\mathrm{T}) \\ \vdots & \ddots & \vdots \\ x_n(0) & \cdots & \mathrm{x}_n(\mathrm{T}) \end{pmatrix}. \quad (2)$$

The T columns of the matrices **X** and **S** represents multiple samples. If the inverse matrix of the mixing matrix A can be obtained, the sources can therefore be recovered.

The BSS can be implemented in two steps. The first is to compute the unmixing matrix W with generalized eigenvalue procedure. Then the sources can be separated as follows [23]:

$$\mathbf{W} = \mathrm{Eig}(\mathbf{X} \cdot \mathbf{X}^{H'}, \mathbf{Q}) \quad (3)$$

$$\hat{\mathbf{S}} = \mathbf{W}^H \mathbf{X} \quad (4)$$

where Q is diagonal cross-statistics that differs depending on the assumptions about the nature of the signals and H is the conjugate transpose operator. As a result of the separation a matrix $\hat{\mathbf{S}}$ is produced which is a scaled and permuted version of **S**.

In [21] for the non-white and non-correlated sources, Q is derived as the symmetric cross-correlation for time-delayed:

$$\mathbf{Q} = \mathbf{X}(0 \ldots T - \tau) \cdot \mathbf{X}^H(\tau + 1 \ldots T) + \mathbf{X}(\tau + 1 \ldots T) \cdot \mathbf{X}^H(1 \ldots T - \tau) \quad (5)$$

where τ is the delay within the non-zero autocorrelation interval in the sources, ant T is the observation time. Equation (5) is used henceforth to perform the signal separation.

Since the separated signals (and hence their powers) are scaled with unknown coefficients they are unsuitable for the TRP contribution measurement. The next section describes how to remove the effect of unknown scaling.

2.2. TRP CONTRIBUTION ESTIMATION

The signal separated by the BSS can be resolved to the actual contribution of the individual sources through an averaging cancellation method, introduced in [19] and [22]. Here a brief summary is repeated.

Let us consider a linear combination of two sources (the case can be easily generalized to an arbitrary number of sources) in the frequency domain:

$$x_1 = k_{11}s_1 + k_{12}s_2 \tag{6}$$

$$x_2 = k_{21}s_1 + k_{22}s_2 \tag{7}$$

where s_1 and s_2 are two source signals, x_1 and x_2 are the probe output signals, and k_{ij} are the transfer functions that represents the signal mixing.

Let us consider now a special case when the probe 2 is coupled only to the source s_2, so $k_{22} = 0$ (in this case the probe 2 is the reference probe with respect to the signal 1). Then the ratio of the probe signals can be written as:

$$\frac{x_1}{x_2} = \frac{k_{11}s_1 + k_{12}s_2}{k_{21}s_1} = \frac{k_{11}}{k_{21}} + \frac{k_{12}s_2}{k_{21}s_1} \tag{8}$$

As demonstrated in [22, (3)-(6)] if the probability distributions of variables s_1 and s_2 are 1) bounded; 2) symmetrical, and the signals are not correlated, the mean value of the ratio (8) is equal to a constant:

$$\left\langle \frac{x_1}{x_2} \right\rangle = \frac{k_{11}}{k_{21}} + \frac{k_{12}}{k_{21}} \left\langle \frac{s_2}{s_1} \right\rangle = \frac{k_{11}}{k_{21}} \tag{9}$$

The averaged amplitude of the contribution of the source s_1 to the probe signal x_1 is equal to $\langle |k_{11}s_1| \rangle$, and therefore the average power in the probe 1 due to source s_1 is:

$$P_{11} = \langle |k_{11}s_1| \rangle^2 \tag{10}$$

At the same time, under the condition $k_{22} = 0$, s_1 can be related to x_2 as follows (using (7)):

$$s_1 = x_2/k_{21} \tag{11}$$

Substituting (11) to (10) the power contribution can be obtained as:

$$P_{11} = \langle |k_{11}x_2/k_{21}\,| \rangle^2 \tag{12}$$

Finally, since, according to (9), $\frac{k_{11}}{k_{12}} = \left\langle \frac{x_1}{x_2} \right\rangle$ the power is:

$$P_{11} = \langle |x_2| \rangle^2 \left| \left\langle \frac{x_1}{x_2} \right\rangle \right|^2 \tag{13}$$

which means that the power contribution can be calculated by multiplying the power in the reference channel $\langle |x_2| \rangle^2$ by the square of the absolute value of the mean of the ratio of the two probe signals.

If the reference signal is available, the formula (13) can be used directly. However, if it is not, the signals can be separated first by the BSS method as described in Section 2, and then the separated signals can be used as references. It should be noted here that the result of (13) does not depend on k_{21} (the transfer coefficient in the reference channel), in other words, the procedure is immune to the arbitrary scaling of the signals during the BSS.

3. TRP MEASUREMENT

3.1. INTRODUCTION OF THE MEASUREMENT SETUP

Figure 1 shows the general measurement setup. The TRP measurement is performed in the reverberation tent, and the setup, in general, corresponds to equations

(6) and (7), with k_{ij} being the transfer coefficients between transmitting and receiving antennas.

Signal generator 1 produces a 1 GHz sinusoidal signal with an amplitude of 5 dBm (Source 1). Signal generator 2 produces a 1.0005 GHz sinusoidal signal with an amplitude of 10 dBm (Source 2). The 500 kHz frequency difference was introduced to be able to discriminate signals in the frequency domain by their phase progressions. Since the signal generators are not referenced to each other, the signals are uncorrelated regardless of the nominal frequency difference. Two log-periodic antennas connected to the outputs of the signal generators are used as emission sources and another two log-periodic antennas are used as receiving probes for the measurement of TRP.

The vector network analyzer is used as the measurement instrument. The center frequency is set to 1 GHz with zero spans. The IF bandwidth is set to 1.5 MHz such that both signals fall into the bandwidth, which makes them indistinguishable in the spectral domain (otherwise the signal separation task could be done trivially just by tuning to the corresponding signal frequencies).

The power calculation procedure explained in a Section 2 assumes that the coefficients k_{ij} are time-invariant. However, in the reverberation tent the transfer coefficients between the antennas are constantly changing due to the movement of the tent's walls. On the other hand, that movement is relatively slow, with typical shaking "period" on an order of a second, or a fraction of a second at worst. As the result, if the averaging in (13) is performed within a short time (relative to the wall movement speed), the transfer coefficients might be treated as quasi-static values. In the measurement, the

sweep time of the VNA was set to 10 ms, which is presumably 10 to 100 times faster than the tent shaking.

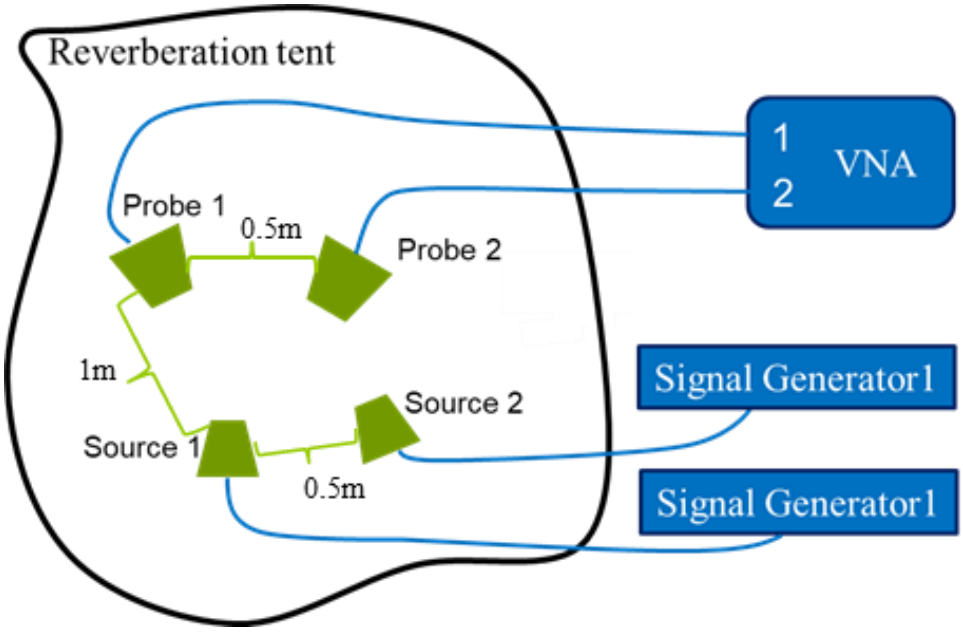

Figure 1. TRP measurement setup: The distance between the probes and the sources is around 1 meter. The distance between the probes and between sources is around 0.5 m.

The signals in two channels must be recorded simultaneously to avoid losing correlations between probe signals x_1 and x_2. For this reason, the number of resolvable sources is practically limited to the number of channels of the measurement instrument.

The total radiated power is estimated by averaging the power (13) over the VNA sweeps (simultaneously with the tent stirring) as:

$$TRP_{11} = \overline{P_{11}} = \overline{\langle |x_2| \rangle^2 \left| \left\langle \frac{x_1}{x_2} \right\rangle \right|^2} \tag{14}$$

where $\langle \cdot \rangle$ represents averaging over all samples within one sweep, and $\bar{\cdot}$ represents averaging over the sweeps.

For validation purposes, the contribution of each source is also measured directly when only one of the signal generators is turned on.

3.2. MEASUREMENT RESULTS

Figure 2 shows the contributions of the sources obtained by measuring the signals when only one of the sources is turned on (measured by one of the probes). The measurements are performed within one 10 ms sweep. As can be seen, the amplitudes are practically time-independent, which demonstrates that the tent can be treated as a time-invariant system within the sweep time (10 ms). The slope of the phases allows to identify signals, i.e. source 1 (1 GHz carrier) has a decreasing phase progression, and source 2 (1.0005 GHz carrier) has an increasing phase progression. In a more practical case of an active electronic devices, signal identification would require detecting signatures in the signals (phase progression, data pattern, etc) which have to be analyzed prior to the TRP measurement. Of identifying signal signatures requires additional investigation and is outside of the scope of this article.

Figure 3 shows the measurement result of the mixed signals (i.e. when both generators are turned on). Compared to the result of the individual source, the amplitude in the probe channels becomes time-dependent (due to beats of two sinusoidal signal with different frequencies). The phase progression loses its linearity.

Figure 4 shows the mean powers in both probe channels measured over 300 sweeps. The power is different for each sweep which is caused by the stirring of the chamber. The average values over the sweeps converge when the chamber is thoroughly stirred [24]. The mean power for Source 1 is -39.6 dBm. The mean power for Source 2 is

-32.1 dBm. The resolving contribution of each source from the mixed signal is expected to have approximately the same level as these.

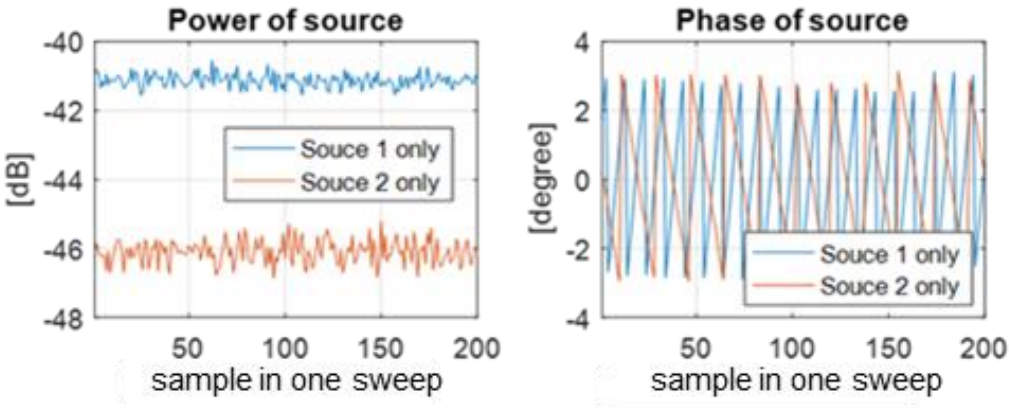

(a) (b)

Figure 2. Power (a) and phase (b) of the individual sources (one sweep).

To resolve the individual contribution of the emission sources, the BSS is applied to the probe signals to obtain the references. An example of the separated signals obtained in one sweep is shown in Figure 5. As can be seen it reproduces the signals in Figure 5 almost perfectly (with respect to unknown scaling), demonstrating successful separation.

The order of the separated result is arbitrary, and the signals are identified by their phase progression.

After achieving the separated results in each sweep using (3) and (4), the average cancellation method (13) is used to calculate the powers of the two signals, and finally the total radiated powers are obtained by averaging over multiple sweeps (14). The

results of this procedure are listed in Table 1. (labeled “resolved”) and compared to the direct TRP measurements.

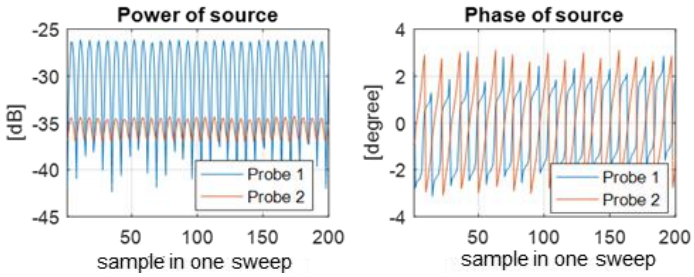

(a) (b)

Figure 3. (a) The Power and (b) the phase of the mixed signals (one sweep).

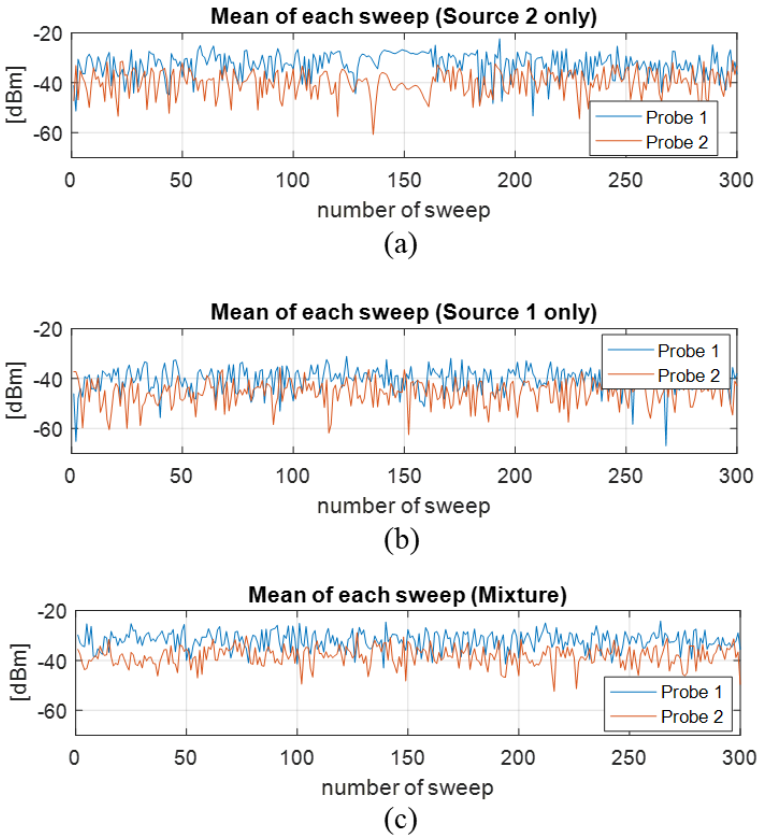

Figure 4. Output amplitude in measurement probes for Source 1 (a), Source 2 (b), mixed case (c) (mean walues within each sweep).

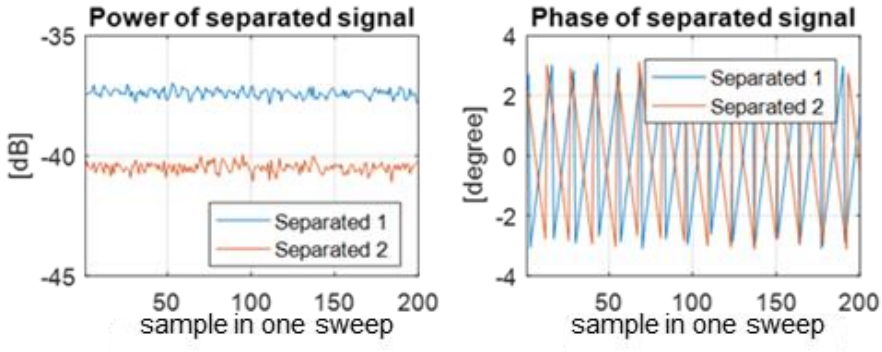

(a) (b)

Figure 5. Amplitude (a) and phase (b) of the resolves signals in one sweep.

Table 1. The amplitude of the TRP contributions measured directly and resolved from the mixture using BSS.

	Source 1	**Source 2**
Direct Measurement	-39.6dBm	-32.1dBm
Resolved	-40.0dBm	-34.9dBm

As can be seen, the resolved results are in good agreement with the ones measured directly. The largest difference (2.8 dB) is observed for the source 2, which is comparable to a typical measurement uncertainty in a reverberation tent.

4. SUMMARY AND CONCLUSIONS

A method is proposed for the total radiated power (TRP) measurement of multiple uncorrelated emission sources in the reverberation tent. The method can resolve the contribution of each source, which is critical to the noise source identification in complex

electronic systems. The TRP contributions can be related to the sources by examining signal signatures (such as phase progression, data pattern, etc). Practical aspects of signal identifications in complex electronic systems deserved additional investigation.

In order to avoid the influence of the tent stirring the BSS is implemented within relatively short time periods.

The BSS result of the mixture can be resolved to the TRP of the individual source through an averaging cancellation method. The method applies for the situation when no access to the sources is available so that all the probes should be placed in the far-field zone. Same method can be applied to the measurements in the conventional reverberation chambers, but without a limitation on the measurement sweep time.

REFERENCES

[1] P. Maheshwari, H. Kajbaf, V. V. Khilkevich and D. Pommerenke, "Emission Source Microscopy Technique for EMI Source Localization," in IEEE Transactions on Electromagnetic Compatibility, vol. 58, no. 3, pp. 729-737, June 2016.

[2] Q. Huang, F. Zhang, T. Enomoto, J. Maeshima, K. Araki and C. Hwang, "Physics-based dipole moment source reconstruction for RFI on a practical cellphone", IEEE Trans. Electromagn. Compat., vol. 59, no. 6, pp. 1693-1700, Dec. 2017.

[3] Q. Huang et al., “Desense Prediction and Mitigation from DDR Noise Source,” in Proc. of IEEE Symp. Electromagn.Compat., 2018, pp. 139-144.

[4] D. Nozadze et al., "Prediction of Worst-Case Radiation Immunity in Cable Harnesses," 2018 IEEE Symposium on Electromagnetic Compatibility, Signal Integrity and Power Integrity (EMC, SI & PI), Long Beach, CA, 2018, pp. 604-609.

[5] G. Maghlakelidze, X. Yan, L. Guan, S. Marathe, Q. Huang, B. Bae, C. Hwang, V.Khilkevich, J. Fan, D. Pommerenke.,“ SNR Analysis and Optimization in Near-Field Scanning and EMI Applications", IEEE Trans. Electromagn. Compat., vol. 60, no. 4, pp. 1087-1094, Aug. 2018.

[6] Q. Huang and J. Fan,“ Machine Learning Based Source Reconstruction for RF Desense", IEEE Trans. Electromagn. Compat., vol. 60, no. 6, pp. 1640-1647, Dec. 2018.

[7] Y. Liu, R. He, V. Khilkevich and P. Dixon, "Shielding Effectiveness of Board Level Shields with Absorbing Materials," 2019 IEEE International Symposium on Electromagnetic Compatibility, Signal & Power Integrity (EMC+SIPI), New Orleans, LA, USA, 2019, pp. 84-89.

[8] Q. Huang, Y. Liu, L. Li, Y. Wang, C. Wu and J. Fan, "Radio frequency interference estimation using transfer function based dipole moment model," 2018 IEEE International Symposium on Electromagnetic Compatibility and 2018 IEEE Asia-Pacific Symposium on Electromagnetic Compatibility (EMC/APEMC), Singapore, 2018, pp. 115-120.

[9] L. Zhang et al., "EMI Coupling Paths and Mitigation in Optical Transceiver Modules," in IEEE Transactions on Electromagnetic Compatibility, vol. 59, no. 6, pp. 1848-1855, Dec. 2017.

[10] J. Li et al., "EMI coupling paths in silicon optical sub-assembly package," 2016 IEEE International Symposium on Electromagnetic Compatibility (EMC), Ottawa, ON, 2016, pp. 890-895.

[11] X. Yang et al., "EMI Radiation Mitigation for Heatsinks Using Characteristic Mode Analysis," 2018 IEEE Symposium on Electromagnetic Compatibility, Signal Integrity and Power Integrity (EMC, SI & PI), Long Beach, CA, USA, 2018, pp. 374-378.

[12] X. Yang et al., "Characterizing Radiation Physics and EMI Mitigation for Heatsinks," 2018 IEEE International Conference on Computational Electromagnetics (ICCEM), Chengdu, 2018, pp. 1-3.

[13] L. Zhang et al., "Sparse Emission Source Microscopy for Rapid Emission Source Imaging," in IEEE Transactions on Electromagnetic Compatibility, vol. 59, no. 2, pp. 729-738, April 2017.

[14] M. Sørensen, H. Kajbaf, V. V. Khilkevich, L. Zhang and D. Pommerenke, "Analysis of the Effect on Image Quality of Different Scanning Point Selection Methods in Sparse ESM," in IEEE Transactions on Electromagnetic Compatibility.

[15] S. Yong, S. Yang, L. Zhang, X. Chen, D. J. Pommerenke and V. Khilkevich, "Passive Intermodulation Source Localization Based on Emission Source Microscopy," in IEEE Transactions on Electromagnetic Compatibility.

[16] J. C. West and C. F. Buntling, "An Analysis of Reverberation Chamber Testing as a Radiation Problem," 2018 IEEE Symposium on Electromagnetic Compatibility, Signal Integrity and Power Integrity (EMC, SI & PI), Long Beach, CA, 2018, pp. 616-621.

[17] P.-S. Kildal and K. Rosengren, “Correlation and capacity of MIMO systems and mutual coupling, radiation efficiency and diversity gain of their antennas: Simulations and measurements in reverberation chamber”, IEEE Communi. Mag., vol. 42, no. 12, pp. 102-112, Dec. 2004.

[18] F. Leferink, J. -. Boudenot and W. van Etten, "Experimental results obtained in the vibrating intrinsic reverberation chamber," IEEE International Symposium on Electromagnetic Compatibility, Washington, DC, 2000, pp. 639-644 vol.2.

[19] A. Patnaik et al., "Source isolation measurements in a multi-source coupled system," 2017 IEEE International Symposium on Electromagnetic Compatibility & Signal/Power Integrity (EMCSI), Washington, DC, 2017, pp. 75-80.

[20] X. Jiao et al., "EMI mitigation with lossy material at 10 GHz," 2014 IEEE International Symposium on Electromagnetic Compatibility (EMC), Raleigh, NC, 2014, pp. 150-154.

[21] W.L.Zhou, D.Chelidze, "Blind source separation-based vibration mode identification, " Mechanical Systems and Signal Processing, Vol.21.Issue. 8. pp.3072-3087. Nov.2007.

[22] T. Li, V. Khilkevich and D. Pommerenke, "Phase-Resolved Near-Field Scan Over Random Fields," IEEE Transactions on Electromagnetic Compatibility, vol. 58, no. 2, pp. 506-511, April 2016.

[23] Lucas. Parra, Paul, Sajda., "Blind source separation via generalized eigenvalue decomposition" The Journal of Machine Learning Research, Vol. 4 Issue 7-8, October 1 - November15, 2004, Pages 1261-1269

[24] Qian Xu; Yi Huang, "Measurement Uncertainty in the Reverberation Chamber," in Anechoic and Reverberation Chambers: Theory, Design, and Measurements, IEEE, 2018, pp.283-303

SECTION

2. CONCLUSIONS

To deal with the electromagnetic interference (EMI) caused by the noise in the EMC measurements, it is of critical importance to identify the emission sources and subtract the noise effect. In complex electronic systems, noise is a product of multiple, often uncorrelated, emission. In a situation with multiple sources knowing the contributions of the individual sources might help to solve the emission problems.

In this thesis, practical methods directly using the measured signal to separate the contribution of the sources are proposed. The separation procedure is based on averaging over realizations. The methods can also deal with the situation that the reference signal with only corrupted by one signal is not available. Blind source separation method can help resolve the reference from the mixture containing unknown, multiple, and overlapping signals.

The methods can be applied in the EMC measurements. For the NFS measurement, the field contributions of the uncorrelated sources are successfully separated and verified. By using the methods, all probes can be placed far away from the sources such that no access to the sources to obtain the reference signals is required. The complexity of the measurement and data processing time are consequently reduced. If the number of sources exceeds the number of probes, the method in its current form will generally fail. However, it still potentially can be used if the number of probes is equal to

the number of dominant sources. The applicability and accuracy of the method, in this case, required additional investigation.

For the TRP measurement, the methods successfully suppress the noise contribution and extend the dynamic range. The BSS result of the mixture can be resolved to the TRP of the individual source through an averaging cancellation method. The methods apply for the situation when no access to the sources is available so that all the probes should be placed in the far-field zone. The same methods can be applied to the measurements in the conventional reverberation chambers, but without a limitation on the measurement sweep time.

The methods can also be applied for the noise cancellation in the future research. In EMC measurements, it is essential to eliminate the effects of wide-spread interference such as Wi-Fi, GSM, FM signals. This is usually achieved by using shielded rooms, however, sometimes the shielding is insufficient (especially in reverberation tents), and additional methods might be needed.

Active noise control and adaptive noise canceling are the two conventional methods to deal with interference in a noisy environment. However, in the EMC measurement, an active noise control method, which needs an additional circuit to generate the canceling signal in the high frequency, is hard to implement. Adaptive noise-canceling removes ambient noise is to use a form of adaptive noise cancellation which usually involving a Weiner filter. Two antennas measure signals simultaneously. The adaptive filter used in this method is trained over successive iterations or generated with the statistics of signal in each block but with increased computational complexity.

Practical methods directly using the measured signal to cancel the noise are proposed. The cancellation procedure is based on averaging over realizations.

The methods can also deal with the situation that the reference signal with only corrupted by the noise signal is not available. Blind source separation method can help resolve the reference from the mixture containing unknown, multiple, and overlapping signals.

VITA

Yuanzhuo Liu received the B.E. degree in electrical and computer engineering from the Huazhong University of Science and Technology, Wuhan, China, in 2017. She worked in electrical engineering from the EMC Laboratory, Missouri University of Science and Technology (formerly University of Missouri-Rolla), Rolla, MO, USA from 2017 to 2019. Her research interests included electromagnetic interference, signal integrity in high-speed digital systems and microwave imaging. She received the Master of Science degree in Electrical Engineering from Missouri University of Science and Technology, USA, in December 2019.